



Eximia Journal
(ISSN 2784-0735)

Vol. 12

2023

Assessing the Impact of COVID-19 Lockdown on Air Pollutants and Wildfires in China

Rida Kanwal, Song Weiguo

University of Science and Technology of China

ridakanwal@mail.ustc.edu.cn, wgsong@ustc.edu.cn

Abstract. This research paper focuses on the impact of COVID-19 lockdown on air pollutants and wildfires in various provinces of China. The study uses machine learning techniques to analyze the association between lockdown restrictions and the subsequent decline in air pollution emissions, which in turn led to a reduction in fire count (FC). The frequency and severity of wildfires have been rising in China, with major negative effects on the country's air quality. Globally unprecedented responses to the COVID-19 epidemic have included lockdowns and limitations on human activity. The purpose of this study is to evaluate how the COVID-19 lockdown has affected air pollutants and wildfires in China. Specially, the focus is on the reduction in ozone (O₃), nitrogen dioxide (NO₂), and carbon monoxide (CO) levels in the air. Satellite images were used before and during the lockdown to gauge the impact. The observed reduction in NO₂, O₃ and CO concentrations during the COVID-19 lockdown demonstrate the potential advantages of taking action to reduce air pollution. The study tries to find connections between the incidence of wildfires and the subsequent emission of air pollutants using machine learning methods. The study creates maps showing the influence of lockdown restrictions on the levels of air pollutants and the number of fires by analyzing historical data on air pollution measurements. These findings highlight the significance of sustainable practices, environmental regulations and offer insightful information regarding the interaction between human activities, air pollutants and wildfires in China.

Keywords. COVID-19, wildfires, air pollutants, machine learning

1. Introduction

The global pandemic of the coronavirus disease (COVID-19) has far-reaching and significant repercussions. The first case was reported to the World Health Organization (WHO) in December 2019 in the Wuhan area of Hubei Province, China [1-2]. A worldwide public health emergency results from its rapid global spread and serious effects [3-4]. Rapid increases in mortality and morbidity rates were accompanied by public health worries, which resulted in "lockdowns" where people's freedom to move around and economic activity was severely constrained to reduce the spread of the disease. Regional and worldwide economies were impacted by the restrictions on industry and transportation caused by the lockdown [5-6]. There have also been reports of decreased levels of noise, air, and water pollution, less waste production, and improved atmospheric visibility as a result of these lockdowns [7-8].

wide range of emission sources, both anthropogenic and natural, have an impact there. Crop residue burning, home heating and cooking, rubbish burning, vehicle emissions, industrial activity, and coal-based power generation are a few examples of anthropogenic sources. Forest fires, the recycling of mineral dust, sea salts, and natural emissions are some of the regional natural sources of emissions.

This non-homogeneous restriction on sectors that pollute the air offers a chance to comprehend the sector-specific impact of various emission sources to the region's air quality across a range of scales from region to country to city. The effects of restricted activity on the economy did not spread evenly across all sectors, with intensive industries like transport being more negatively impacted than the residential sector.

The lockdown caused a 10–31% GDP decline, or a loss of 30–921 billion dollars [16], mostly due to restrictions on the power, industry, and transportation sectors. Hence, presenting a chance to comprehend the potential of putting mitigation measures in place in these areas and its associated expenses. This study employed satellite imagery to classify and create maps, enabling a comprehensive analysis of air pollutant levels before and during the lockdown period across different provinces in China. The primary objective was to assess the impact of reduced emissions on air pollutants and examine how this reduction correlated with a decrease in the number of wildfires. By utilizing these maps, a clearer understanding of the relationship between emissions, air pollution, and fire occurrences was obtained.

3. Materials and Methods

In this study, we quantify the impact of COVID-19 and associated restriction on levels of gaseous pollutants over the selected China provinces domain using satellite imagery. The analysis period was 1st January-30th April 2019–1st and January-30th April 2020, which includes approximately 1 year of data prior to the implementation of COVID-19 restrictions and 4 months of continuous data under more complete national lockdowns. Exact dates for lockdown implementation varied from province to province (see Table 1) [17]. To maintain consistency the period 1st January-30th April 2019 was selected as the pre-lockdown period, with the 1st January-30th April 2020 period was designated as the during lockdown period. Selected satellite data for 2020 in general and the study period in particular were compared with available data from 2000–2019. Most China provinces have limited ground-based observations of air pollutants. To overcome this, multiple satellite based remote sensing products were used.

Table 1: List of lockdown implementation timeline in different provinces.

Province	COVID-19 Lockdown	
	Start date	End date
Hebei	2/7/2020	3/18/2020
Shandong	2/3/2020	2/9/2020
Gansu	2/7/2020	3/18/2020
Henan	2/4/2020	4/10/2020
Jiangsu	2/4/2020	2/8/2020
Shaanxi	2/3/2020	2/9/2020
Anhui	2/3/2020	3/18/2020
Hubei	2/1/2020	3/22/2020
Sichuan	2/5/2020	3/18/2020

Zhejiang	2/2/2020	2/8/2020
Jiangxi	2/4/2020	3/31/2020
Hebei	2/7/2020	3/18/2020
Guizhou	2/7/2020	3/18/2020
Guangdong	2/6/2020	3/18/2020

3.1. Moderate Resolution Imaging Spectroradiometer (MODIS)

The Terra and Aqua Satellite platforms were launched in 1999 and 2002, respectively, and placed into solar synchronous polar orbits. These satellites are equipped with MODIS multispectral instruments, which enable the continuous measurement of aerosols and clouds. In this study, we utilized the daily atmospheric pollutant data obtained from the Sentinel-5p satellite, specifically focusing on NO₂, O₃ and CO. Additionally, we collected daily fire data from MODIS for the periods of 1st January-30th April, 2019 and 1st January-30th April, 2020. The concentration data for NO₂, O₃ and CO were derived from the Sentinel-5 Precursor satellite (<https://scihub.copernicus.eu/>). The European Space Agency launched the Sentinel-5 Precursor satellite on October 13, 2017, with the primary purpose of monitoring air pollution. In this study, we utilized data from Sentinel-5 Precursor to track and analyze air pollution levels. Additionally, we incorporated MODIS active fire products to obtain information regarding the timing and geographical distribution of large-scale fires in the area [18-19].

3.2. TROPospheric Monitoring Instrument (TROPOMI)

The European Space Agency launched the TROPOMI spectrometer aboard the Sentinel-5 Precursor (S-5 P) mission. This single payload satellite operates in a sun-synchronous orbit. TROPOMI is designed to capture data across various spectral ranges, including ultraviolet (UV), visible (VIS), near-infrared (NIR), and shortwave infrared (SWIR) [20]. The TROPOMI spectrometer provides daily global coverage, capturing data at a spatial resolution of 7 × 7 km² and a swath width of 2600 km. To determine the total column density of carbon monoxide (CO), TROPOMI measures the Earth's radiance spectra within the 2.3 μm spectral range of the shortwave infrared (SWIR) region [21-22]. For this study, we utilized the Level 3, Offline (OFFL) CO dataset for the years 2019 and 2020. The dataset was obtained from the data catalog of the Google Earth Engine platform. It is important to note that the availability of the dataset was limited due to the age of the satellite used [23].

4. Results and Discussion

4.1. Sources of pollution in China

The rapid industrialization and urbanization that China has experienced in recent decades have resulted in increased energy consumption and intensified pollution levels. Additionally, the burning of fossil fuels, such as coal, for electricity generation and heating purposes, contributes significantly to air pollution. The presence of air pollution in China can be attributed to a diverse array of sources, both natural and human-related, which exhibit notable fluctuations across various timeframes.

To assess the effects of COVID-19 restrictions on air pollutants, it is crucial to comprehend the prevailing emission scenarios within the study area. This study examines the remotely sensed data of FC as well as concentrations of three air pollutants (NO₂, O₃ and CO) during two time periods: 1st January to 30th April, 2019, and 1st January 1st to 30th April, 2020.

Additionally, the correlation between FC and air pollutant concentration is investigated across various provinces in China.

4.2. Impact of lockdown on air pollutants in China

In this study, the impact of the lockdown on air pollutant levels is examined in two ways (a) a comparison is made between air pollutant levels during the lockdown period and those observed in the pre-lockdown period, (b) the correlation between FC and air pollutant concentrations. To conduct the analysis, available datasets for each pollutant from the years 2019 and 2020 are utilized as the pre-lockdown reference data.

4.3. Comparison of air pollutants between Pre and during lockdown period

Fig. 2 (left panel) shows the pre-lockdown period (1st January-30th April 2019) satellite-derived data of NO₂, O₃ and CO. because of better understating of the spatial distribution of the pollutants across China during this period (pre-lockdown period) was deemed necessary to examine the impact of lockdown imposed in 2020. The other data for the year 2020 (Fig. 2, right panel) represents the air pollutants levels during the COVID-19 forced lockdown period (1st January-30th April 2020), and the difference between pre-lockdown data and post-lockdown data displays the changes of levels in air pollutants due to lockdown.

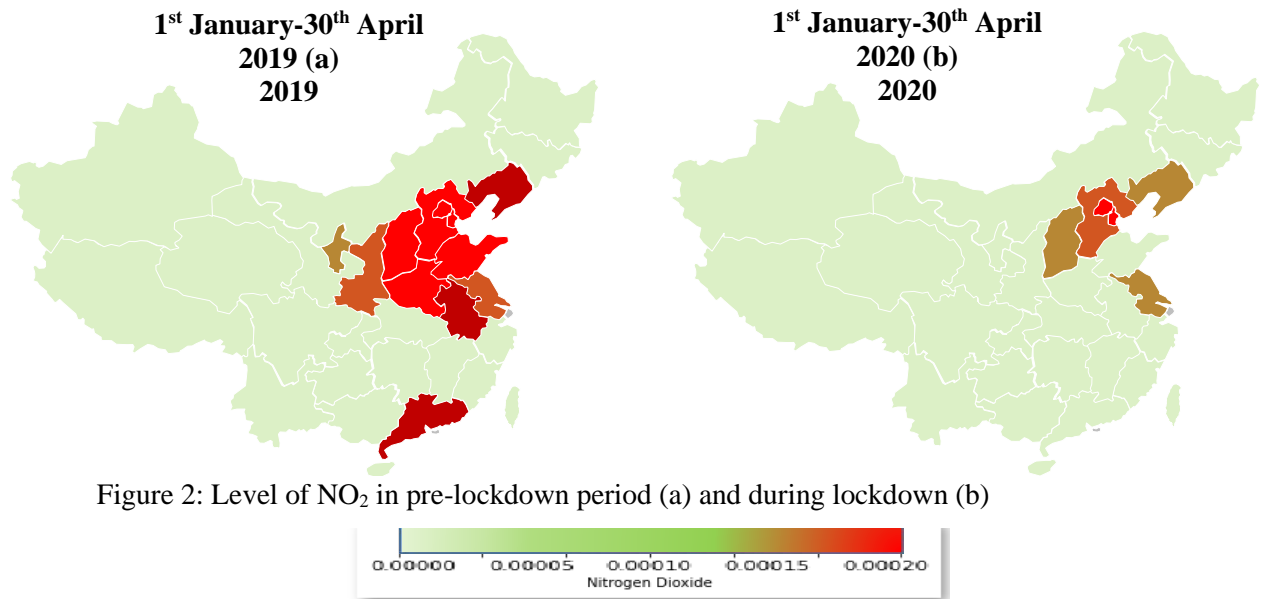


Figure 2: Level of NO₂ in pre-lockdown period (a) and during lockdown (b)

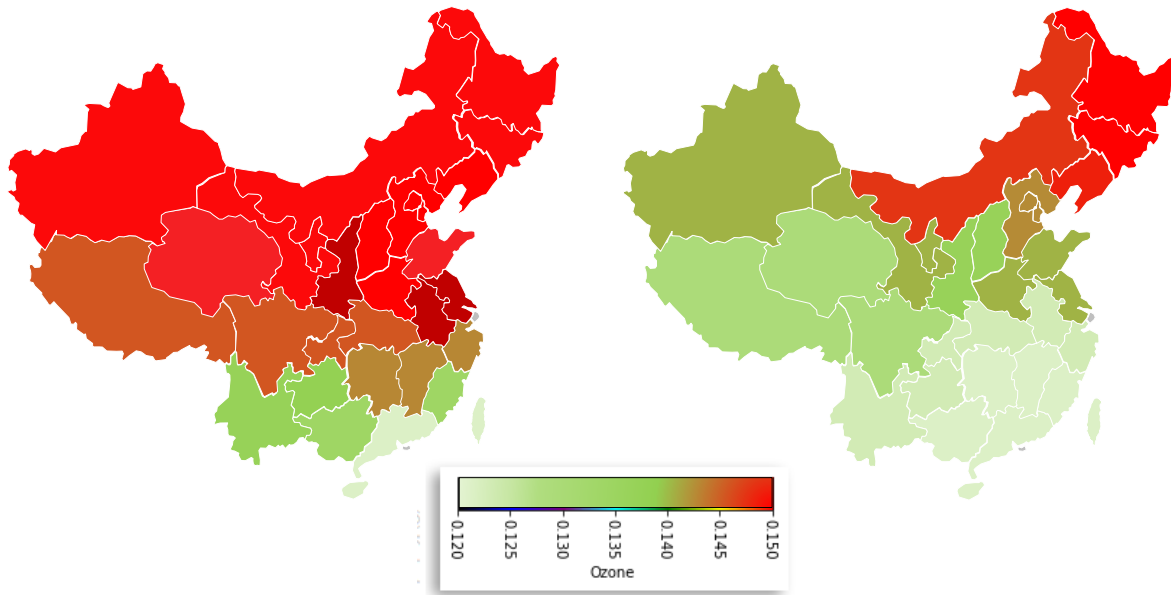


Figure 3: Level of O₃ in pre-lockdown period (a) and during lockdown (b)

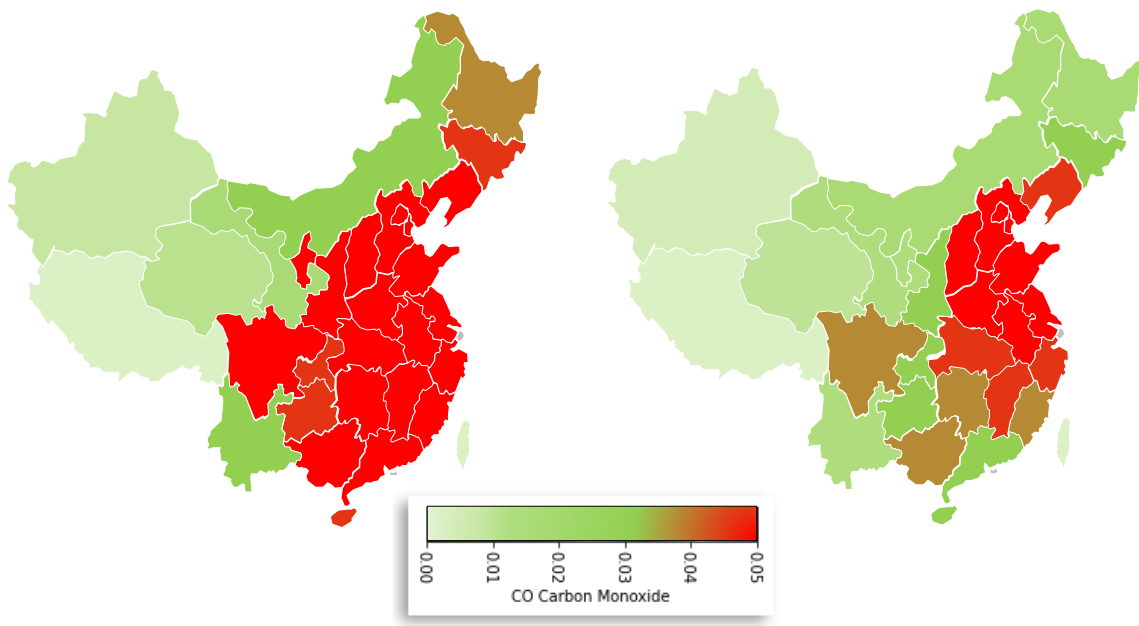


Figure 4: Level of CO in pre-lockdown period (a) and during lockdown (b)

Pre-lockdown data shows that O₃ was usually high over the eastern part of China due to its high population density, residential and industrial emissions and forest fires (Fig. 5). In general, the O₃ over western also remains high throughout the year and exhibits a west to east transition depending on the seasons. O₃ gradually decreases while moving towards the north, west and east to south. In contrast to widely distributed O₃ over China, NO₂ and CO are showing decreasing trend over distinct hotspots. It is a guess that high NO₂ levels are found increased in

2019 over cities because of vehicular emissions, whereas high CO levels are found increased because of industrial zones and power plant locations. Open burning also contributes total NO₂ emission over China hence NO₂ hotspots are also observed in the forest fire dominated eastern part of the China. Over China, the pre-lockdown level of NO₂, O₃ and CO was 0.000125-0.000200, 0.145-0.150 and 0.02-0.05 respectively. While that for the year 2020 was 0.000100-0.000200, and 0.140-0.150 and 0.01-0.05, respectively. However, NO₂ levels after lockdown nearly zero.

During the period of lockdown, notable changes in air pollutant levels were observed across different regions of China. The concentration of CO exhibited a decrease from the northern to the western parts of the country, while an increase was observed in the eastern and southern provinces (Fig. 4). Similarly, there was a decrease in NO₂ levels in the northwestern and southern regions, while an increase was observed in eastern China (Fig. 2). Furthermore, a reduction in O₃ levels was observed in the majority of provinces across China, except for a significant increase observed in the northeast and northern regions (Fig.3). In specific provinces within the northeast region, an increase in NO₂ levels was also observed, along with patches of high CO concentrations. This area is known for its significant industrial activity, including power generation plants and mining operations. The spatial distribution of O₃ showed an overall increase across most regions of China, with a higher increase observed in the northeast and northwest parts of the country. These findings highlight the regional variations in air pollutant levels during the lockdown period, with different pollutants exhibiting distinct patterns across different provinces and regions of China.

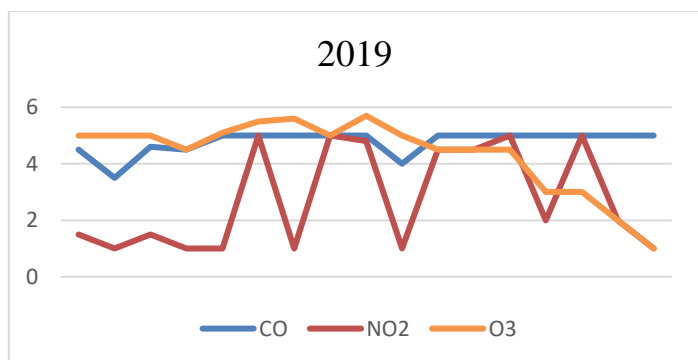


Figure 5: Line plot for a level of air pollutants in pre-lockdown period over Hebei, Shanxi, Shandong, Gansu, Henan, Jiangsu, Shaanxi, Anhui, Hubei, Sichuan, Zhejiang, Jiangxi, Hunan, Guizhou, Fujian, Guangdong, and Guangxi provinces of China

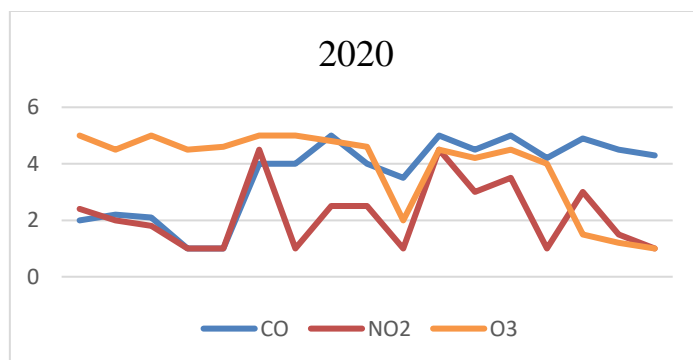


Figure 6: Line plot for a level of air pollutants during lockdown period over Hebei, Shanxi, Shandong, Gansu, Henan, Jiangsu, Shaanxi, Anhui, Hubei, Sichuan, Zhejiang, Jiangxi, Hunan, Guizhou, Fujian, Guangdong, and Guangxi provinces of China

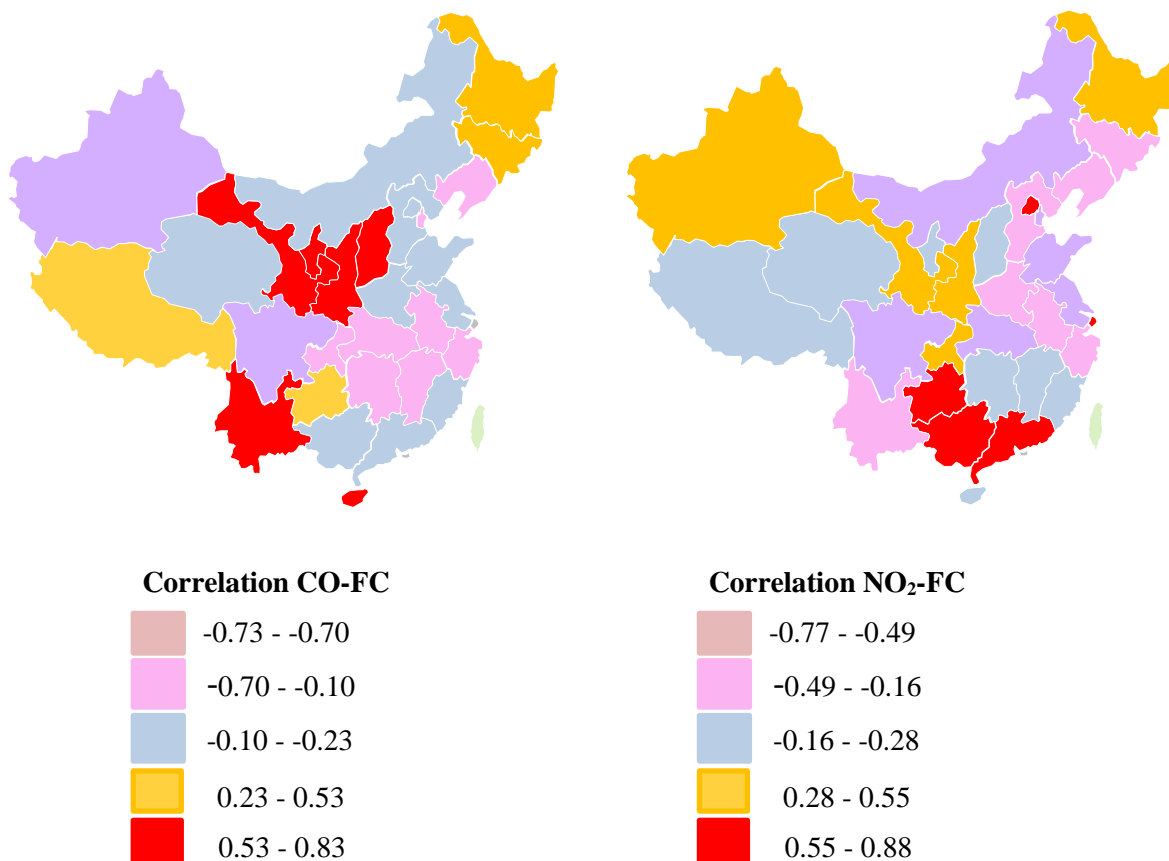
The study compared satellite-derived data for NO₂, O₃, and CO during the lockdown period with the data from the pre-lockdown period. The comparison was made for different provinces in China, and the results are presented in Figure 5 and 6. On a provincial scale, the analysis revealed a decrease in NO₂, O₃, and CO levels during the lockdown period compared to the pre-lockdown period. Specifically, in the months of January to April, the provinces of Hebei, Shanxi, Shandong, Gansu, Henan, Jiangsu, Henan, Shaanxi, Anhui, Hubei, Sichuan, Zhejiang, Jiangxi, Hunan, Guizhou, Fujian, Guangdong, and Guangxi experienced a reduction of 1.5% in NO₂ levels, 1.5% in O₃ levels, and 3.9% in CO levels. These findings suggest that

the implementation of the lockdown measures had a positive impact on reducing air pollutant levels in these provinces during the specified time period.

4.4. Correlation between FC and air pollutants

Monthly, O₃ shows positive correlation with FC. Based on the figure 7, +0.91 to +0.94, indicating a positive relationships between the O₃ and FC. A positive correlation is indicated by positive values (e.g., +0.91, +0.92) and suggests that as O₃ increases, the number of FC tends to increase as well. Based on the figure 7, it can be concluded that CO, NO₂ and FC show a negative correlation. This is indicated by the negative values (e.g., -0.73, -0.70, -0.10, -0.23) in the CO-FC pair and (e.g., -0.77, -0.49, -0.16) in the NO₂-FC pair. Negative correlation between CO, NO₂ and FC means that as CO and NO₂ decreases, the number of FC also tends to decrease. In other words, there is an inverse relationship between CO and NO₂ levels and the occurrence of fires. This suggests that higher levels of CO and NO₂ are associated with a higher number of FC, while lower levels of CO and NO₂ are associated with a lower number of FC.

Understanding the correlation between FC and air pollutants is crucial for assessing the impact of pollution on fire occurrence. It suggests that reducing CO, NO₂ and O₃ emissions can help mitigate the risk of fires.



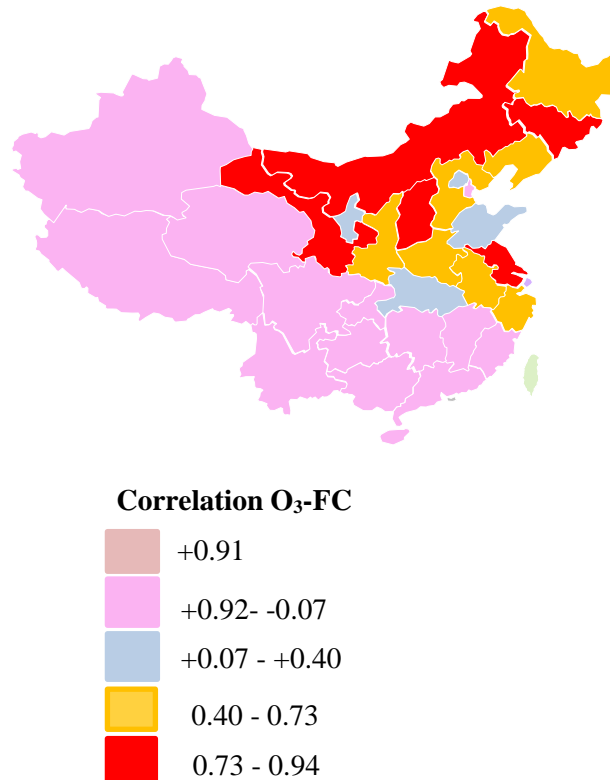


Figure 7: Correlation between FC and air pollutants (CO and NO₂ and O₃)

Conclusions

This study provides evidence of a decrease in air pollutant levels (specifically NO₂, O₃, and CO) across China during the designated lockdown period from (1st January–30th April 2020). The analysis conducted at the provincial level revealed a decline in the levels of NO₂, O₃, and CO, which corresponded to a decrease in the number of FC. These findings suggest a strong correlation between FC and air pollutant concentrations.

In this study, we conducted a comprehensive exploration of the usefulness of air pollutant data derived from Sentinel 5P Data in illuminating and simulating the spatial distribution of FC across China. The findings of our study indicate a close relationship between the variations in FC and air pollutant levels, with generally positive correlations observed in the monthly observations. When comparing different provinces, we observed a stronger association between FC and air pollutants in the southwestern provinces of China.

Overall, this study presents compelling evidence that a substantial decrease in emissions from vehicles and industries, comparable to the levels witnessed during the lockdown period, can effectively lead to a significant reduction in the number of FC at the provincial level.

The implications of this study hold significant importance for policymakers and environmental agencies, emphasizing the need to prioritize sustainable practices and enforce stricter regulations to curb emissions and enhance air quality. By taking such measures, not only can the risk of fires be effectively mitigated, but it will also lead to a reduction in overall environmental and public health impacts.

Acknowledgments: The work was supported by National Key R&D Program of China (2021YFC3000300).

References

- [1] Li, Q., Guan, X., Wu, P., Wang, X., Zhou, L., Tong, Y., Ren, R., Leung, K.S.M., Lau, E.H.Y., Wong, J.Y., Xing, X., Xiang, N., Wu, Y., Li, C., Chen, Q., Li, D., Liu, T., Zhao, J., Liu, M., Tu, W., *et al.* (2020). Early Transmission Dynamics in Wuhan, China, of Novel Coronavirus–Infected Pneumonia. *N. Engl. J. Med.* 382, 1199–1207. <https://doi.org/10.1056/NEJMoa2001316>
- [2] WHO Newsroom (2020). WHO Timeline - COVID-19. World Health Organization.
- [3] Lai, C.C., Shih, T.P., Ko, W.C., Tang, H.J., Hsueh, P.R. (2020). Severe acute respiratory syndrome coronavirus 2 (SARS-CoV-2) and coronavirus disease-2019 (COVID-19): The epidemic and the challenges. *Int. J. Antimicrob. Agents* 55, 105924. <https://doi.org/10.1016/j.ijantimicag.2020.105924>
- [4] Phua, J., Weng, L., Ling, L., Egi, M., Lim, C.M., Divatia, J.V., Shrestha, B.R., Arabi, Y.M., Ng, J., Gomersall, C.D., Nishimura, M., Koh, Y., Du, B. (2020). Intensive care management of coronavirus disease 2019 (COVID-19): Challenges and recommendations. *Lancet Respir. Med.* 8, 506–517. [https://doi.org/10.1016/S2213-2600\(20\)30161-2](https://doi.org/10.1016/S2213-2600(20)30161-2)
- [5] International Centre for Integrated Mountain Development (ICIMOD) (2020). COVID-19 impact and policy responses in the Hindu Kush Himalaya. International Centre for Integrated Mountain Development, Kathmandu, Nepal. <https://doi.org/10.53055/ICIMOD.2>
- [6] World Bank (2020). Global Economic Prospects, June 2020. World Bank, Washington, DC. <https://doi.org/10.1596/978-1-4648-1553-9>
- [7] McNeill, V.F. (2020). COVID-19 and the air we breathe. *ACS Earth Space Chem.* 4, 674–675. <https://doi.org/10.1021/acsearthspacechem.0c00093>
- [8] Zambrano-Monserrate, M.A., Ruano, M.A., Sanchez-Alcalde, L. (2020). Indirect effects of COVID-19 on the environment. *Sci. Total Environ.* 728, 138813. <https://doi.org/10.1016/j.scitotenv.2020.138813>
- [9] [World Health Organization \(WHO\) \(2022\). Ambient air pollution data.](#)
- [10] Fattorini, D., Regoli, F. (2020). Role of the chronic air pollution levels in the Covid-19 outbreak risk in Italy. *Environ. Pollut.* 264, 114732. <https://doi.org/10.1016/j.envpol.2020.114732>
- [11] Sharma, S., Zhang, M., Anshika, Gao, J., Zhang, H., Kota, S.H. (2020b). Effect of restricted emissions during COVID-19 on air quality in India. *Sci. Total Environ.* 728, 138878. <https://doi.org/10.1016/j.scitotenv.2020.138878>
- [12] Venter, Z.S., Aunan, K., Chowdhury, S., Lelieveld, J. (2020). COVID-19 lockdowns cause global air pollution declines with implications for public health risk (preprint). *Epidemiology* <https://doi.org/10.1101/2020.04.10.20060673>
- [13] Kanniah, K.D., Kamarul Zaman, N.A.F., Kaskaoutis, D.G., Latif, M.T. (2020). COVID-19's impact on the atmospheric environment in the Southeast Asia region. *Sci. Total Environ.* 736, 139658. <https://doi.org/10.1016/j.scitotenv.2020.139658>
- [14] Menut, L., Bessagnet, B., Siour, G., Mailler, S., Pennel, R., Cholakian, A. (2020). Impact of lockdown measures to combat Covid-19 on air quality over western Europe. *Sci. Total Environ.* 741, 140426. <https://doi.org/10.1016/j.scitotenv.2020.140426>
- [15] Song, Rong, et al. "Spatial and temporal variation of air pollutant emissions from forest fires in China." *Atmospheric Environment* 281 (2022): 119156.

- [16] Kanitkar, T. (2020). The COVID-19 lockdown in India: Impacts on the economy and the power sector. *Glob. Transitions* 2, 150–156. <https://doi.org/10.1016/j.glt.2020.07.005>
- [17] *COVID-19 lockdown in China - Wikipedia*. (2022, November 1). COVID-19 Lockdown in China - Wikipedia. https://en.wikipedia.org/wiki/COVID-19_lockdown_in_China
- [18] Giglio, L., Descloitres, J., Justice, C.O., Kaufman, Y.J. (2003). An enhanced contextual fire detection algorithm for MODIS. *Remote Sens. Environ.* 87, 273–282. [https://doi.org/10.1016/S0034-4257\(03\)00184-6](https://doi.org/10.1016/S0034-4257(03)00184-6)
- [19] Justice, C.O., Giglio, L., Korontzi, S., Owens, J., Morisette, J.T., Roy, D., Descloitres, J., Alleaume, S., Petitcolin, F., Kaufman, Y. (2002). The MODIS fire products. *Remote Sens. Environ.* 83, 244–262. [https://doi.org/10.1016/S0034-4257\(02\)00076-7](https://doi.org/10.1016/S0034-4257(02)00076-7)
- [20] Veeffkind, J.P., Aben, I., McMullan, K., Förster, H., de Vries, J., Otter, G., Claas, J., Eskes, H.J., de Haan, J.F., Kleipool, Q., van Weele, M., Hasekamp, O., Hoogeveen, R., Landgraf, J., Snel, R., Tol, P., Ingmann, P., Voors, R., Kruizinga, B., Vink, R., *et al.* (2012). TROPOMI on the ESA Sentinel-5 Precursor: A GMES mission for global observations of the atmospheric composition for climate, air quality and ozone layer applications. *Remote Sens. Environ.* 120, 70–83. <https://doi.org/10.1016/j.rse.2011.09.027>
- [21] Fu, D., Bowman, K.W., Worden, H.M., Natraj, V., Worden, J.R., Yu, S., Veeffkind, P., Aben, I., Landgraf, J., Strow, L., Han, Y. (2016). High-resolution tropospheric carbon monoxide profiles retrieved from CrIS and TROPOMI. *Atmos. Meas. Tech.* 9, 2567–2579. <https://doi.org/10.5194/amt-9-2567-2016>
- [22] Landgraf, J., Aan De Brugh, J., Scheepmaker, R., Borsdorff, T., Hu, H., Houweling, S., Butz, A., Aben, I., Hasekamp, O. (2016). Carbon monoxide total column retrievals from TROPOMI shortwave infrared measurements. *Atmos. Meas. Tech.* 9, 4955–4975. <https://doi.org/10.5194/amt-9-4955-2016>
- [23] Gorelick, N., Hancher, M., Dixon, M., Ilyushchenko, S., Thau, D., Moore, R. (2017). Google Earth Engine: Planetary-scale geospatial analysis for everyone. *Remote Sens. Environ.* 202, 18–27. <https://doi.org/10.1016/j.rse.2017.06.031>